THE JOURNAL OF BIOLOGICAL CHEMISTRY VOL. 287, NO. 34, pp. 28456–28469, August 17, 2012

The Stoichiometric Transition from Zn_6Cu_1-Metallothionein to Zn_7-Metallothionein Underlies the Up-regulation of Metallothionein (MT) Expression

QUANTITATIVE ANALYSIS OF MT-METAL LOAD IN EYE CELLS[*] [S]

Received for publication, April 2, 2012, and in revised form, June 19, 2012 Published, JBC Papers in Press, June 21, 2012, DOI 10.1074/jbc.M112.365015

Lydia Alvarez[‡1], Hector Gonzalez-Iglesias[‡1], Montserrat Garcia[‡], Sikha Ghosh[§], Alfredo Sanz-Medel[¶], and Miguel Coca-Prados[‡§2]

From the [‡]Fundación de Investigación Oftalmológica, Instituto Oftalmológico Fernández-Vega, 33012 Oviedo, Spain, the [§]Department of Ophthalmology and Visual Science, Yale University School of Medicine, New Haven, Connecticut 06510, and the [¶]Department of Physical and Analytical Chemistry, University of Oviedo, 33006 Oviedo, Spain

Background: Metallothioneins (MTs) and immune responses are induced by exogenous zinc.
Results: MTs are abundant and differentially expressed in human ocular tissues. A bioanalytical hybrid technique provided absolute measurements of MT-metal loads in cultured cells.
Conclusion: Zinc stimulated the transition of Zn_6Cu_1-MT to Zn_7-MT and blocked proinflammatory cytokines in cultured eye cells.
Significance: Zn_7-MT species may confer protective antioxidative effect.

We examined the profiling of gene expression of metallothioneins (MTs) in human tissues from cadaver eyes with microarray-based analysis. All MT1 isoforms, with the exception of MT1B, were abundantly expressed in lens and corneal tissue. Along with MT1B, MT4 was not detected in any tissues. Antibodies to MT1/2 labeled the corneal epithelial and endothelial cells, whereas MT3 label the retinal ganglion cells. We studied the effects of zinc and cytokines on the gene expression of MT isoforms in a corneal epithelial cell line (HCEsv). Zinc exerted an up-regulation of the expression of MT isoforms, and this effect was further potentiated in the presence of IL1α or TNFα. Zinc also elicited a strong down-regulation of the expression of inflammatory cytokines, and this effect was blocked in the presence of TNFα or IL1α. The concentration of MTs, bound zinc, and the metal stoichiometry of MTs in cultured HCEsv were determined by mass spectrometry. The total concentration of MTs was 0.24 ± 0.03 μM and, after 24 h of zinc exposure, increased to 0.96 ± 0.01 μM. The combination of zinc and IL1α further enhanced the level of MTs to 1.13 ± 0.03 μM. The average metal stoichiometry of MTs was Zn_6Cu_1-MT, and after exposure to the different treatments, it changed to Zn_7-MT. Actinomycin D blocked transcription, and cycloheximide attenuated synthesis of MTs in the presence or absence of zinc, suggesting transcriptional regulation. Overall the data provide molecular and analytical evidence on the interplay between zinc, MTs, and proinflammatory cytokines in HCEsv cells, with potential implications on cell-based inflammatory eye diseases.

Metallothioneins (MTs)[3] are cytosolic zinc ion-binding proteins of low molecular mass (6–7 kDa) that exhibit a diverse range of functions, including promoting neuroprotection (1, 2), cellular zinc homeostasis, and defense against oxidative damage and inflammation. MTs consist of two domains. The α-domain (32–61 residues) binds four zinc ions and contains 11 cysteinyl residues, whereas the β-domain (1–31 residues) binds 3 zinc ions and contains 9 cysteinyl residues. Together they form two metal/thiolate clusters (3). MT proteins bind heavy metals, both physiological (*i.e.* zinc or copper) and xenobiotic (*i.e.* cadmium, mercury, silver, and arsenic) through thiol groups present in 20 cysteine residues (~30%). The MT family consists of multiple isoforms grouped into four groups (1–4) that share a high degree of homology at the nucleotide and amino acid levels. MT1 and MT2 are abundantly expressed in many tissues, MT3 is expressed in the CNS and in the retina, and MT4 is found in stratified tissues (3). There are at least eight functional isoforms within the MT1 group (MT1A, MT1B, MT1E, MT1F, MT1G, MT1H, MT1M, and MT1X). All the MTs differ by a small number of amino acids in their amino acid sequence (4). Moreover, MT3 presents two insertions of six and one amino acid respectively in its sequence, and MT4 contains an insertion of only one amino acid. The reason for this high diversity of MT isoforms is currently unknown. MT1 and MT2 can be induced *in vivo* by factors including zinc (5),

* This work was supported in part by a CENIT-CeyeC Research Grant CEN-20091021 from the Spanish Ministry of Innovation and Development, Fundación de Investigación Oftalmológica Fernández-Vega, Fundación Mª Cristina Masaveu Paterson, and Fundación Rafael del Pino.
[S] This article contains supplemental Figs. S1–S5 and Tables S1–S4.
[1] Both authors contributed equally to this work.
[2] Catedratico Rafael del Pino en Oftalmología in the Fundación de Investigación Oftalmológica, Instituto Oftalmológico Fernández-Vega, Oviedo, Spain. To whom correspondence should be addressed: Dept. of Ophthalmology and Visual Science, Yale University School of Medicine, 300 George St., R8100A, New Haven, CT 06510. Tel.: 203-785-2742; Fax: 203-785-7401; E-mail: Miguel.Coca-Prados@yale.edu.

[3] The abbreviations used are: MTs, metallothioneins; AMD, age-related macular degeneration; ICP-MS, inductively coupled plasma mass spectrometry; RPE, retinal pigment epithelium; ActD, actinomycin D; CH, cycloheximide; SEC, size exclusion chromatography; AEC, anionic exchange chromatography; IPD, isotope pattern deconvolution.

glucocorticoids (6), cytokines such as IL-6 and TNFα (7–9), and regulatory response elements in their genes (10).

The antioxidant functions of MTs reside on their capacity to capture and neutralize free radicals during oxidative stress through cysteine sulfur ligands of MT oxidation (11–13). This property is likely linked to their ability to bind zinc and serve as zinc-ion donors in a redox-dependent fashion in cellular biological processes (14, 15). Therefore, MTs display a key role in intracellular zinc homeostasis. Zinc is an essential element in the cell that serves as a catalytic cofactor to enzymes, a structural component of proteins, and is involved in many cellular processes including gene expression (16). Although zinc itself does not exhibit redox properties, it can exert important effects in the redox metabolism of the cell. Thus, a deficiency or an excess of zinc within cells can lead to cell death; however, within physiological concentrations, zinc exhibits pro-antioxidant properties (17). It is generally accepted that cellular homeostasis of zinc is strictly regulated by zinc transporters and zinc-binding proteins, which are capable of binding and transferring zinc ions to other proteins (18).

In the eye MTs have been suggested to play a key role in protection of neuronal retinal cells and act as endogenous antioxidants (19). Zinc has also been associated with age-related macular degeneration (AMD) in a major clinical study called Age-Related Eye Disease Study. In this study it was shown that therapy of AMD that included antioxidants and zinc supplementation significantly reduced the progression of the neovascular form of AMD in patients at intermediate and late stages (20). However, precisely how zinc supplementation helps to slow down the progression of AMD is not quite understood at the cellular and molecular levels. It has been speculated that aging is associated with a deficiency in zinc, leading to chronic inflammation and oxidative stress in the immune system (21, 22). Likewise, zinc supplementation was associated with higher protection against protein oxidation (23). Others studies have shown evidence supporting the view that zinc modulates the cellular immune function of T-cells via cytokine signaling (24).

Only a few limited studies have been designed to investigate the role of zinc in the human eye and its effects on MTs and cellular immune signaling. To better understand the role of zinc binding MT proteins in the eye, we first examined by array analysis the gene expression profiling of MT isoforms in normal human eye donors (cadavers) and compared their abundance between tissue types (*i.e.* cornea, trabecular meshwork, lens, iris, ciliary body, retina, retinal pigment epithelium, and sclera).

Second, we used an *in vitro* cell culture model (HCEsv cell line), representative of the human corneal epithelium, to examine the mechanism(s) regulating MT gene expression. The useful aspect of this cell line is its capacity to mimic the profiling of gene expression with intact tissue (*i.e.* cornea), which included the co-expression of multiple MT isoforms and of pro- and anti-inflammatory cytokines. This property makes the cell line an attractive *in vitro* model for addressing questions related to zinc effects on MT isoforms and cytokine expression at the mRNA and protein levels in the absence of immune cells (*i.e.* T and B cells).

Third, we applied analytical and biochemical techniques, including high performance liquid chromatography (HPLC), inductively coupled plasma mass spectrometry (ICP-MS), and matrix-assisted laser desorption ionization time of flight (MALDI-TOF), to determine the "absolute" concentration of zinc-bound MTs and bound zinc in HCEsv cells under steady-state conditions and upon treatment with exogenous zinc. Recent studies have validated the ICP-MS as a powerful technique to determine the absolute concentration of proteins in biological fluids, meaning absolute the quantitation of protein without a relative comparison (25).

In this work we present the first evidence of the general profiling of gene expression of multiple MT isoforms in ocular tissues from human eye donors and their complex mechanisms of regulation by exogenous zinc and cytokines. In addition, we demonstrate the use of analytical technologies to study the homeostasis of zinc-bound MTs by agents known to modulate their expression.

EXPERIMENTAL PROCEDURES

Tissue RNA Extraction

A total of 12 eyes from adult normal donors (cadavers) ranging in age from 66 to 80 years old were used in this study. Eyes were obtained 24 h postmortem through the National Disease Research Interchange (Philadelphia, PA). The procedures conformed to the tenets of the Declaration of Helsinki. The RNA was isolated from cornea, trabecular meshwork, iris, lens, ciliary body, retina, retinal pigment epithelium (RPE), and sclera, with TRIzol® reagent (Invitrogen) and further purified with RNeasy Mini Kit (Qiagen, Hilden, Germany). The RNA concentration and quality was determined using a bioanalyzer (Agilent 2100 Bioanalyzer, Agilent Technologies Inc., Santa Clara, CA).

Microarray Analysis of Human Metallothioneins

RNA samples from 11 corneas, 9 trabecular meshworks, 11 irises, 10 lenses, 12 ciliary bodies, 12 retinas, 8 RPEs, and 7 scleras with RNA Integrity Number scores above 7.5 were further processed individually to examine the whole-genome expression profiling using the Illumina BeadChip array platform (HumanHT-12 v4.0 Expression BeadChip kit) (Illumina, San Diego, CA). cRNA labeling and hybridization to the chip and array data analysis were carried out at the Genome Analysis Platform (CIC bioGUNE, Derio, Spain).

Raw data from each of the microarrays was normalized, and the background was subtracted. The quantile value for each of the multiple MT isoforms (MT1A, MT1B, MT1E, MT1F, MT1G, MT1H, MT1M, MT1X, MT2A, MT3, and MT4) was determined, and the mean value in every ocular tissue assayed is shown in supplemental Fig. 1.

RNA Extraction from Cultured Cells

Total RNA was also isolated from a human cornea cell line, HCEsv (Riken BIOSOURCE Center, Tokyo, Japan), using TRIzol® reagent (Invitrogen), and the profile of MT gene expression was assayed using the Illumina BeadChip array platform as indicated for ocular tissues.

Immunohistochemistry

The cellular distribution of MT proteins in whole human eye sections was visualized by indirect immunofluorescence. Eyes from donors (cadavers) were formalin-fixed and paraffin-embedded after conventional protocols. Sections (5 μm thick) from fixed and paraffin-embedded blocks were de-paraffinized and stained with a mouse monoclonal antibody to MT1/2 (ab12228, Abcam) or with a rabbit polyclonal antibody to MT3 (HPA004011, Sigma). Tissue sections were incubated overnight at 4 °C with the primary antibodies (dilution 1:100 and 1:200, respectively), rinsed in PBS, and further incubated with the secondary antisera (1:200-fold-diluted, rhodamine-conjugated goat anti-mouse IgG, or rhodamine-conjugated goat anti-rabbit IgG) for 60 min. After washing in PBS and mounting in a solution of glycerol mounting medium, the images were captured with a Leica DM6000 microscope equipped with epifluorescence, a DFC310 Fx Leica camera, and the AF6000 advanced fluorescent software (Leica Microsystems CMS GMBH, Germany). The cellular distribution of MT1/2 and MT3 antibodies in the human cornea and retina, respectively, are shown in supplemental Figs. 2 and 3.

Cell Line, Culture Conditions, and Cellular Treatments

A human cornea cell line, HCEsv, was purchased (Riken BIOSOURCE Center, Tokyo, Japan) and used to study the effects of zinc and cytokines on MTs gene expression. HCEsv cells were cultured in Dulbecco's modified Eagle's medium/nutrient mixture F-12 (DMEM/F-12, Invitrogen) containing 7.5% fetal bovine serum (v/v) at 37 °C and 5% CO_2. Twenty-four hours before each treatment, cells were washed twice with phosphate-buffered saline (PBS), and the serum-containing medium was replaced by the serum-free medium EX-CELL™ Hybridoma (Sigma). Then cultured cells were treated with either 1) $^{68}ZnSO_4$ (100 μM) (Isoflex), 2) IL-1α (100 units/ml) (Millipore), 3) $^{68}ZnSO_4$ (100 μM) + IL-1α (100 units/ml), 4) TNFα (50 units/ml) (Sigma), or 5) $^{68}ZnSO_4$ (100 μM) + TNFα (50 units/ml) for periods of time that ranged from 24, 48, or 72 h as described in each experiment. Each experiment was carried out in triplicate.

Enriched Stable Isotopes

Stable isotope solution enriched in ^{34}S (99.61% abundance of ^{34}S), ^{67}Zn (94.01% abundance of ^{67}Zn), and ^{111}Cd (96.25% abundance of ^{111}Cd) were purchased from Cambridge Isotope Laboratories (Andover, MA). ^{65}Cu (90.03% abundance of ^{65}Cu) was purchased from Spectrascan (Teknolab AS Dröbak, Norway). ^{68}Zn (99.23% abundance of ^{68}Zn) was purchased from Isoflex (San Francisco, CA). The isotopically enriched zinc sulfate solution ($^{68}ZnSO_4$) used for cell culture treatment was prepared from elemental ^{68}Zn by dissolving the metal in a minimum volume of supra-pure grade H_2SO_4 and then diluting with ultrapure water. The isotopic measurements were carried out on an Element 2 sector field (SF)-ICP-MS unit (Thermo Fisher Scientific, Bremen, Germany). Plasma operating conditions and acquisition parameters are shown in supplemental Table 1.

Cellular Labeling of MTs with the Enriched Stable Zinc Isotope (^{68}Zn), and MT Extraction

The ^{68}Zn tracer was added as $^{68}ZnSO_4$ (100 μM) in the culture medium of HCEsv cells during cell stimulation to favor its binding to zinc binding proteins including MTs. HCEsv cells were grown in DMEM/F-12 culture medium to semiconfluency, washed twice with PBS, and further incubated in EX-CELL™ Hybridoma medium for 24 h in the presence or absence of $^{68}ZnSO_4$ (100 μM) or $^{68}ZnSO_4$ (100 μM) + IL1α (100 units/ml). Next the cellular MT proteins were extracted.

For cellular MT extraction, cultured HCEsv cells were washed 3 times with PBS, trypsinized, and collected by centrifugation at 200 × *g* for 5 min. The cell pellet was resuspended in 1.0 ml of TRIS buffer (10 mM, pH 7.4, and degassed under N_2 atmosphere), and cells were disrupted with an ultrasonic cell disintegrator (Bandelin sonoplus HD2070, Berlin, Germany) on ice at 10 KHz for 30 s 3 times at 30-s intervals as previously described (26). The cellular homogenate was centrifuged for 20 min at 16,000 × *g*, and the supernatant (cytosolic fraction) and the pellet were saved and stored at −80 °C for further MT analysis (see below). Oxygen was avoided during the storage of the cytosolic fractions (by internal atmosphere of nitrogen and Teflon insulation) to prevent oxidation of MTs through cysteinyl residues.

Inhibition of Transcription and Protein Synthesis in HCEsv Cells

Cultured HCEsv cells were pretreated for 30 min with either 10 μM actinomycin D (ActD, transcription inhibitor) or 1 μM cycloheximide (CH, protein synthesis inhibitor), both purchased from Sigma, followed by $^{68}ZnSO_4$ (100 μM) or $^{68}ZnSO_4$ (100 μM) + IL1α (100 units/ml) treatments for 24 h.

Fractionation of the Cytosolic Fraction from Cultured HCEsv Cells

A HPLC system (Shimadzu, model LC-20AD, Kyoto, Japan) equipped with a Rheodyne six-port injector and fitted with a 50-μl sample loop and the corresponding column (size exclusion chromatography (SEC) or anionic exchange chromatography (AEC) columns, see below) was used. A scavenger column (25 × 0.5-mm inner diameter) packed with Kelex-100 (Schering, Germany) and impregnated with silica C18 material was placed between the pumps and the injection valve to remove metal ions present in the mobile phases.

Fractionation by SEC—A SEC column, Superdex 200 10/300 GL (Amersham Biosciences), was employed for the chromatographic separation (based on the molecular weight) of the cytosolic fraction of HCEsv cells. Fifty microliters (20–35 μg of protein) of the soluble cell extract were injected in the column and fractionated following the conditions shown in supplemental Table 1 as previously described (27).

Orthogonal Fractionation by AEC—The MTs fraction collected after SEC in a parallel experiment was lyophilized and adjusted to pH 7–7.4 for further injection (50 μl) on an anionic exchange column, Mono Q 5/50 GL (Amersham Biosciences). For gradient elution and buffers see supplemental Table 1.

Two different standard markers were used. The first was for calibration of the SEC column and consisted of a mixture of the following species: thyroglobulin, IgG, ovalbumin, myoglobin, and vitamin B12. A second standard was used to determine the

retention time of human MTs in SEC and AEC columns and consisted of a mixture of MT1A (Zn_7-MT-1A, human) and MT2A (Zn_7-MT-2A, human) proteins, obtained from Bestenbalt LLC (Tallinn, Estonia).

Identification of MTs Proteins

Mass Determination and Tryptic Analysis—Aliquots (60 μg of protein) of the cytosolic fraction from cultured HCEsv cells treated with $^{68}ZnSO_4$ (100 μM) (see "Cellular Labeling of MTs with the Enriched Stable Zinc Isotope (^{68}Zn), and MT Extraction") were injected (up to 5 times in separate experiments) on the SEC column, and the fractions corresponding to MTs (7–14 KDa) were collected, lyophilized, and resuspended in Milli-Q water (100 μl). This "MT-enriched fraction" was subdivided in two aliquots; one aliquot was used for mass determination and the other for tryptic analysis (modified trypsin was obtained from Pierce), peptide MS measurement, and MALDI-TOF analysis as previously described in Wang *et al.* (28).

MALDI-TOF Analysis—An aliquot of 0.5 μl of the eluted MT-protein/peptides fraction was mixed on a MALDI plate with α-cyano-4 hydroxycinnamic acid matrix solution (Applied Biosystems, Foster city, CA) following the sample preparation recommended by Shimadzu Biotech. Sample analysis was carried out in a Voyager-De STR (Applied Biosystems, Langen, Germany) as previously described (27).

Quantification of Total Zinc, Copper, and Cadmium Levels in the Cytosolic and Insoluble Fractions of HCEsv Cells

Quantifications of zinc, copper, and cadmium in the cytosolic and insoluble fractions of HCEsv cells were carried out by flow injection analysis. Before analysis, the insoluble fraction was completely solubilized (mineralized) by a mixture of HNO_3 and H_2O_2 (supra-pure quality) and sonicated for 15 min. The resulting solution was diluted with Milli-Q water (1:1). The elemental isotopic composition in each injected sample was measured by online flow injection analysis-ICP-MS.

Quantification of Sulfur-, Copper-, and Cadmium-binding Proteins in the Cytosolic Fraction of HCEsv Cells by Isotope Dilution-HPLC-ICP-MS

The quantification of these elements in the cytosolic fraction was carried out by online post-column isotope dilution analysis, widely described in previous reports (29–32). The enriched stable isotopes ^{34}S, ^{65}Cu, and ^{111}Cd contained in a solution at standardized concentration were added after the chromatographic separation (for quantitative speciation). The continuous measurement of the corresponding isotope ratios $^{32}S/^{34}S$, $^{63}Cu/^{65}Cu$, and $^{114}Cd/^{111}Cd$ in the ICP-MS allowed us to obtain the "mass flow chromatogram" after applying the isotope dilution equation application (29). Integration of the area under each chromatographic peak provided the absolute mass for these elements: sulfur, copper, and cadmium.

Quantification of Zinc-binding Proteins, Including MTs, in the Soluble Fraction of HCEsv Cells by Isotope Pattern Deconvolution (IPD)-HPLC-ICP-MS; Natural (^{nat}Zn) and Exogenous Zinc (^{68}Zn) Differentiation

The concentration of zinc-binding proteins in HCEsv cells (cytosolic and insoluble fractions) were determined by IPD.

$$\begin{bmatrix} {}^{64}A_b \\ {}^{66}A_b \\ {}^{67}A_b \\ {}^{68}A_b \\ {}^{70}A_b \end{bmatrix} = \begin{bmatrix} {}^{64}A_{nat} & {}^{64}A_{68} & {}^{64}A_{67} \\ {}^{66}A_{nat} & {}^{66}A_{68} & {}^{66}A_{67} \\ {}^{67}A_{nat} & {}^{67}A_{68} & {}^{67}A_{67} \\ {}^{68}A_{nat} & {}^{68}A_{68} & {}^{68}A_{67} \\ {}^{70}A_{nat} & {}^{70}A_{68} & {}^{70}A_{67} \end{bmatrix} \times \begin{bmatrix} X_{{}^{nat}Zn} \\ X_{{}^{68}Zn} \\ X_{{}^{67}Zn} \end{bmatrix} + \begin{bmatrix} {}^{64}e \\ {}^{66}e \\ {}^{67}e \\ {}^{68}e \\ {}^{70}e \end{bmatrix}$$

EQUATION 1

This is a chemometric technique based on multiple least squares for isolating distinct isotope signatures from mixtures of natural abundances and enriched tracers (33). This mathematical tool, in connection with ICP-MS and stable isotopes, has already been applied for the quantification of selenium and iron (34, 35) and sulfur-containing biomolecules (32) and finding distribution of zinc in navy beans (36). We present here for the first time a novel approach to distinguish ^{nat}Zn from tracer ^{68}Zn in cell extracts from cultured cells and a method to determine the total concentration of intracellular MTs after cell exposure with $^{68}ZnSO_4$.

In the present technique, samples containing ^{nat}Zn and ^{68}Zn were spiked at the beginning of the analysis with enriched ^{67}Zn (quantitation tracer). The tracer ^{68}Zn derived from $^{68}ZnSO_4$ when used in tracer experiments (*i.e.* cultured HCEsv cells labeled with $^{68}ZnSO_4$). The relative abundance of each of the zinc isotopes in the sample under analysis was determined by using matrix Equation 1. In this equation, A represents the relative abundance of the distinct zinc isotopes (^{64} Zn, ^{66}Zn, ^{67}Zn, ^{68}Zn, and ^{70}Zn), and the variables x_{natZn}, X_{68Zn}, and x_{67Zn} correspond to the molar fractions of ^{nat}Zn, ^{68}Zn, and ^{67}Zn present in the biological sample and calculated by least square minimization of the error vector "e." Once the molar fractions were calculated by the multivariate linear regression, the total amounts of ^{nat}Zn and ^{68}Zn could be determined, as the amount of ^{67}Zn added was known (34).

Absolute Quantification and Determination of Stoichiometry of MTs in HCEsv Cells

Based on the fact that the number of sulfur atoms per MT molecule is known to be 21 and information gathered from the quantification of sulfur, zinc, copper, and cadmium in the MT protein by isotope dilution and IPD mathematical approaches, we were able to determine the stoichiometry of these elements bonded to MT proteins in the soluble protein fraction of HCEsv cells (37). For this purpose we used the enriched stable isotopes sulfur (^{34}S), zinc (^{67}Zn), copper (^{65}Cu), and cadmium (^{111}Cd) to determine the sulfur and metal content following procedures previously described (4, 30, 37).

RESULTS

Clustering Gene Expression of MT Isoforms in the Human Eye—A hierarchical cluster analysis, heatmap, (ArrayStar software, Version 4 (DNASTAR, Inc, Madison, WI) was performed to allow visual differentiation of signal from noise of the MT isoforms expressed in every human ocular tissue assayed by microarray (see "Experimental Procedures").

The hierarchical ranking and clustering of the MTs genes is shown in Fig. 1. Four clusters could be distinguished (A, B, C, and D), each containing genes expressed at levels ranging from

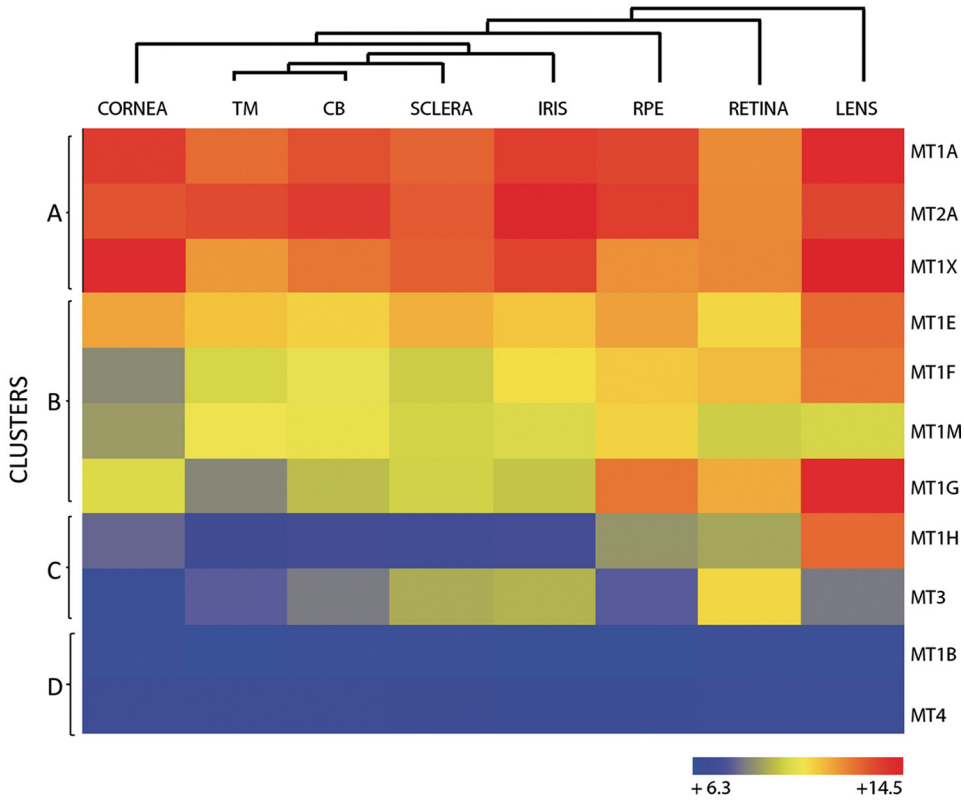

FIGURE 1. **Hierarchical cluster and heatmap of MT isoforms in human ocular tissues.** The *row at the top* shows the clustering information in the form of a dendogram and the similarity relationships among the genes and tissues: cornea, trabecular meshwork (*TM*), ciliary body (*CB*), sclera, iris, RPE, retina, and lens. The *column at the left* of the heatmap shows four clusters (*A–D*), each with MT isoforms expressed at different abundance, from high to low. Mean values of 7–12 biological replicas per tissue are indicated according to the log2 scale, in arbitrary units, depicted at the *bottom*.

highly abundant (*i.e.* cluster A) to moderate (*i.e.* cluster B), low (*i.e.* cluster C), and absent (cluster D). Genes in cluster A (MT1A, MT2A, and MT1X) were highly expressed in all the tissues but in particular in lens, cornea, and iris. Genes in cluster B (MT1E, MT1F, MT1M, and MT1G) were expressed in much lower levels than those in cluster A, with the exception of MT1G that was expressed abundantly in lens. Genes in cluster C (MT1H and MT3) were expressed at low levels but were restricted preferentially to the lens and retina, respectively. Finally, genes in cluster D (MT1B and MT4) were undetected by microarray.

To validate the gene expression of MTs obtained by microarray analysis, we performed quantitative real-time PCR on at least one RNA sample of each eye tissue assayed. The relative abundance of MTs detected was comparable with those found by microarray analysis (data not shown).

Responses of Cultured HCEsv Cells to Zinc; Up-regulation of MT Gene Expression and Down-regulation of Cytokinetic Gene Expression, Respectively—The finding that the human cornea expressed abundant levels of MT isoforms and that corneal epithelial cells were immunolabeled with MT1/2 antibodies (see supplemental Fig. 2) prompted us to explore whether a commercially available human corneal epithelial cell line (HCEsv) could be used as an *in vitro* cell model to study the mechanisms of MT gene expression and regulation.

We used microarray analysis to determine the profile of gene expression of MT isoforms in cultured HCEsv cells, first, under steady-state conditions, and then, upon treatment up to 48 h with agents known to modulate MT expression, including $^{68}ZnSO_4$ and proinflammatory cytokines (*i.e.* IL1α and TNFα). These results are shown in Figs. 2, *panels A* and *B*, and 3. The results can be summarized as follows. (i) Under control conditions, cultured HCEsv cells express MT isoforms in the order of abundance MT2A > MT1A > MT1X > MT1E > MT1F > MT1G > MT1H > MT1B) (Fig. 2, *panels A* and *B*); (ii) upon exposure to $^{68}ZnSO_4$ (100 μM), HCEsv cells responded with a robust up-regulation of the gene expression of MT isoforms, ranging from 3-fold on MT1X to 25-fold on MT1H (Fig. 2, *panels A* and *B*); (iii) $^{68}ZnSO_4$ (100 μM) elicited a down-regulation of the gene expression of pro- and anti-inflammatory cytokines, including IL6 (2-fold) and IL8 (3-fold) (Fig. 3); (iv) $^{68}ZnSO_4$ (100 μM) when added in combination with IL1α (100 units/ml) or TNFα (50 units/ml) (*i.e.* $^{68}ZnSO_4$ + IL1α, $^{68}ZnSO_4$ + TNFα) further potentiated the up-regulation of MT gene expression by up to 40% (*i.e.* MT1G) (Fig. 2) but failed to down-regulate the gene expression of cytokines (*i.e.* IL6 and IL8), respectively (Fig. 3); (v) TNFα (50 units/ml) and IL1α (100 units/ml) when added alone, enhanced the expression of other cytokines (*i.e.* IL8), ranging from to 3.7-fold by IL1α to 7.9-fold by TNFα (Fig. 3).

It is of interest to mention that the expression of MT1M in cornea was absent in cultured HCEsv cells or after different cell treatments. In contrast, MT1B that was not present in the native tissue (cornea), was induced by zinc in cultured HCEsv cells. Furthermore, genes within the MT1 group, in particular MT1B, -1E, -1F, -1G, -1H, and -1X, were highly induced in the

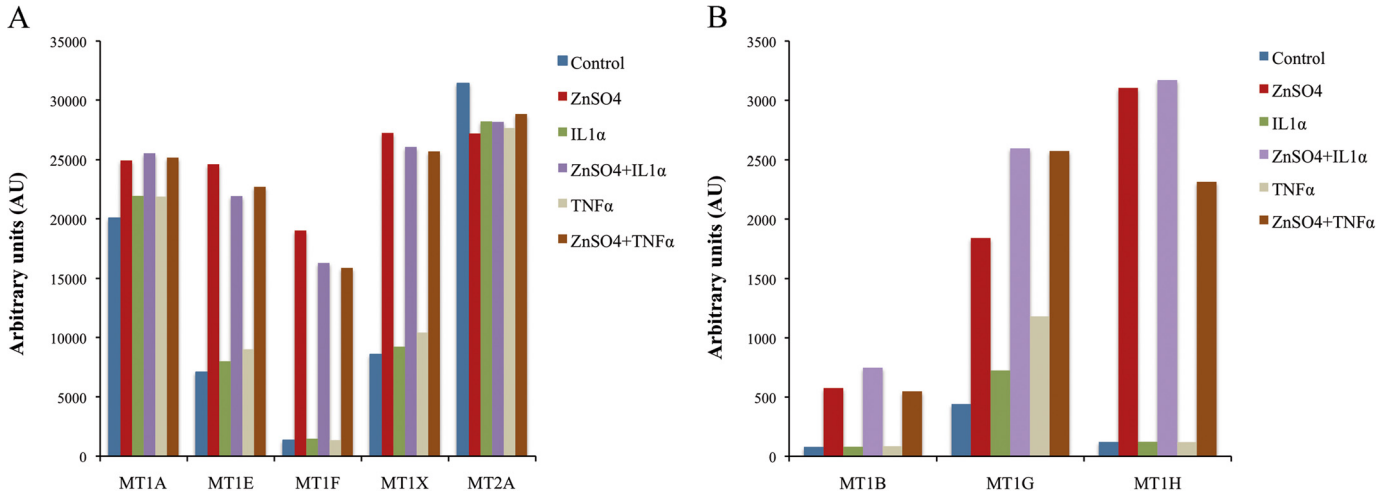

FIGURE 2. ***A* and *B*, microarray analysis of the multiple metallothionein isoforms expressed in cultured HCEsv cells before (*Control*) and after being exposed for 48 h with either (i) $ZnSO_4$, (ii) IL1α, (iii) $ZnSO_4$ + IL1α, (iv) TNFα, or (v) $ZnSO_4$ + TNFα.** The relative hybridization signal obtained for each of the MT isoforms was normalized with internal controls and expressed as arbitrary units. *AU*, arbitrary units. *Panel A* shows the profiling of MT isoforms MT1A, MT1E, MT1F, MT1X, and MT2A, and *panel B* shows the profiling of MT1B, MT1G, and MT1H.

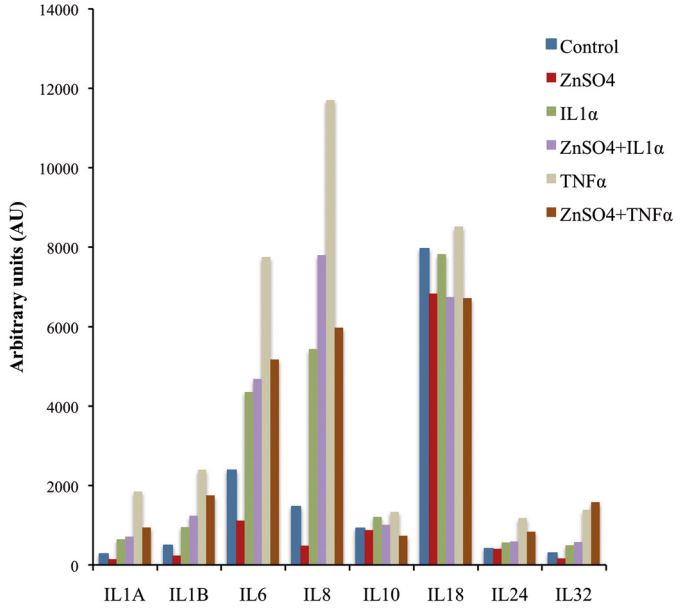

FIGURE 3. **Microarray analysis of cytokines expressed in cultured HCEsv cells under control conditions (no treatment) and after being exposed for 48 h with either (i) $ZnSO_4$, (ii) IL1α, (iii) $ZnSO_4$ + IL1α, (iv) TNFα, or (v) $ZnSO_4$ + TNFα.** The relative hybridization signal obtained for each cytokine analyzed was normalized with internal controls and expressed as arbitrary units. *AU*, arbitrary units.

presence of zinc or in combination with cytokines. The above data were also validated by quantitative real-time PCR. Although PCR was found to be more sensitive than microarray-based technology, the data indicated comparable results (data not shown).

Identification of MT Proteins and Effects of Exogenous Zinc ($^{68}ZnSO_4$) and IL1α on MT Protein Synthesis and Metal Binding—To verify whether the up-regulation of MT gene expression induced by $^{68}ZnSO_4$ and cytokines in cultured HCEsv cells correlated with an increase in MT proteins, we first applied HPLC-ICP-MS to separate MTs present in the cytosol (soluble protein fraction) from other zinc-binding proteins in HCEsv cells. Second, we identified the MT proteins by MALDI-TOF-MS analysis.

By size exclusion chromatography coupled to ICP-MS, we were able to separate ^{nat}Zn from ^{68}Zn bound to MTs and other zinc-binding proteins (distinct to MTs). Under control conditions (no treatment), the ^{nat}Zn tracer was bound to two main peaks (Fig. 4). One peak had a retention time between 25 and 28 min that matched with the retention time of commercially purified MT proteins (7–14 kDa) run in parallel. A second peak, with a retention time between 28 and 32 min, likely corresponded to zinc binding species (*i.e.* bioligands, biomolecules) with a molecular mass smaller than 7 kDa. Finally, a very small third peak was detected with a retention time between 10 and 15 min that likely corresponded to zinc bound to other zinc-binding proteins (>14 kDa) not related to MTs (Fig. 4, *panel A*).

Upon treatment of cultured HCEsv cells with $^{68}ZnSO_4$ (100 μM) (Fig. 4, *panel B*) or with $^{68}ZnSO_4$ (100 μM) + IL1α (100 units/ml) (Fig. 4, *panel C*), the MT-bound tracers of ^{68}Zn (*dashed line*), and ^{nat}Zn (*solid line*) exhibited the same retention time (25–28 min) but different concentrations. The ^{68}Zn tracer associated to the 7–14-kDa material increased significantly upon $^{68}ZnSO_4$ or $^{68}ZnSO_4$+IL1α treatments when compared with the concentration of the tracer ^{nat}Zn under the same treatment or to the concentration of ^{nat}Zn bound to MTs in control. Finally, the exposure of HCEsv cells with IL1α (100 units/ml) elicited a moderate but significant increase in the concentration of ^{nat}Zn in MTs (Fig. 4, *panel D*).

To verify that the molecular mass and protein composition of the $^{nat}Zn/^{68}Zn$-bound proteins (separated by size exclusion chromatography ICP-MS with the retention time between 25 and 28 min) were enriched with MT proteins, they were subjected to MALDI-TOF analysis. We first obtained the spectra of the undigested material and revealed three peaks. The main peak exhibited an experimental molecular mass of 6042.92 Da, very close to the theoretical molecular mass of 6042.16 Da assigned to the human MT2A isoform (see supplemental Fig. 4*A*). The MALDI-TOF analysis of the same material after tryptic digestion provided a mass spectrum shown in supplemental Fig. 4*B*. A search of the Swiss-Prot protein data base using the program Mascot suggested that main peptide mass mapping

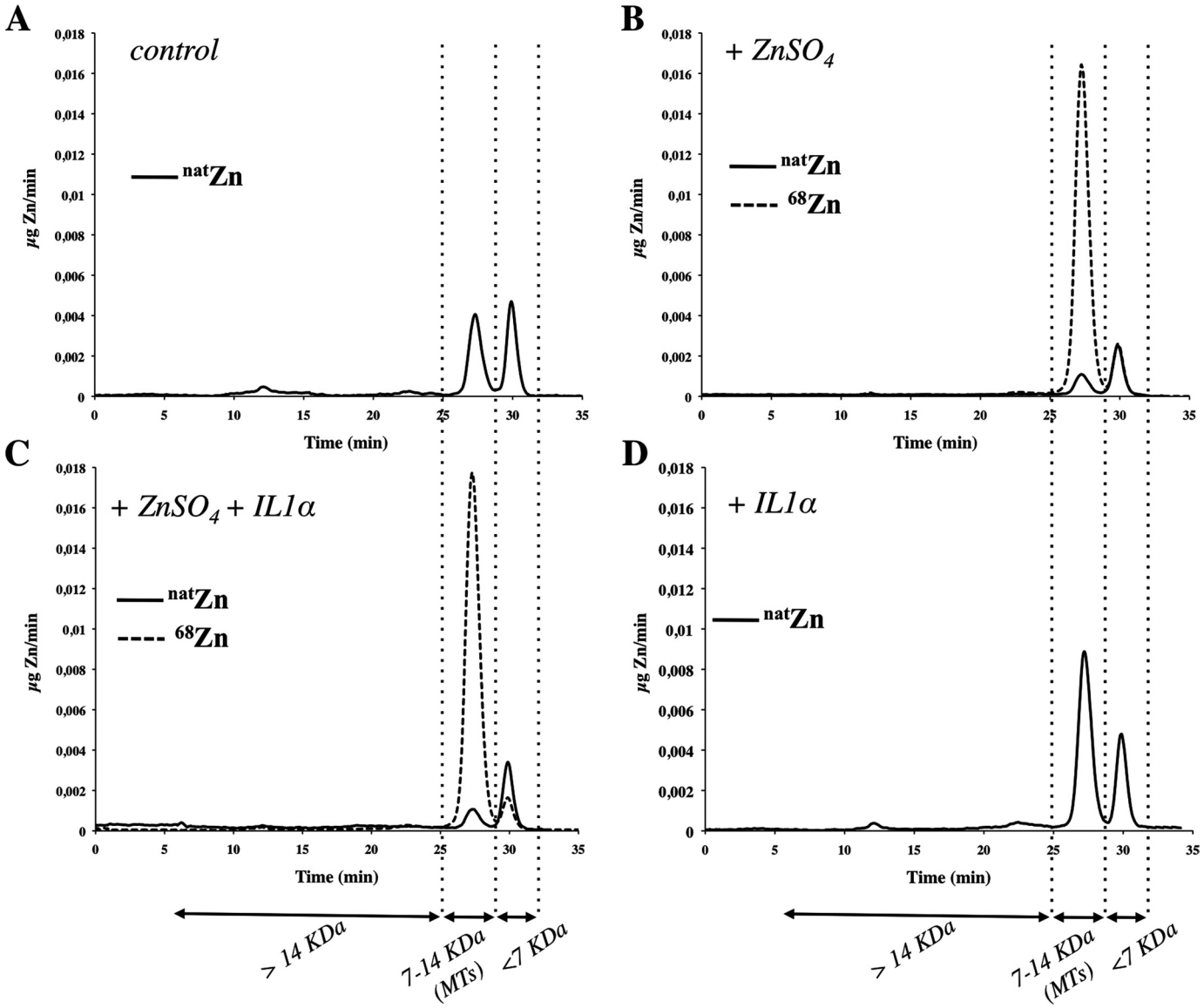

FIGURE 4. ***A–D*, mass flow chromatograms of the zinc tracers, natural zinc (^{nat}Zn) (*solid line*) and exogenous zinc (^{68}Zn) (*dashed line*), bound to proteins including MTs (expressed as µg/min) in the soluble fractions of cultured HCEsv cells by size exclusion-IPD-ICP-MS.** *Panels A–D* are highlighted with *vertical dotted lines*, the predicted size (7–14 kDa) and time of exclusion (between 25 to 28 min) of zinc-labeled MTs and zinc binding material with relative masses smaller than 7 kDa (<7 kDa) and a time of exclusion between 28 to 32 min, respectively. The time of exclusion between 0 to 25 min represents zinc-binding proteins with a relative mass bigger than 14 kDa (> 14kDa). *Panel A*, HCEsv cells under control conditions (no treatment); *panel B*, after 24 h of treatment with $^{68}ZnSO_4$; *panel C*, after 24 h of treatment with $^{68}ZnSO_4$ + IL1α; *panel D*, after 24 h or treatment with IL1α.

analysis corresponded to MT2A, with the highest sequence coverage (65%) and a score of 52. Lower sequence coverage (32%) and a score of 30 could be also assigned to other MT isoforms including MT1X and MT1G. Thus these analyses confirmed that ^{68}Zn and ^{nat}Zn are preferentially bound to MTs, of which MT2A appeared to be the predominant isoform present in HCEsv-cultured cells.

Once we verified and confirmed the identity of MT proteins, we were able to determine the concentrations of ^{nat}Zn, ^{68}Zn, and ^{nat}Zn+^{68}Zn associated to these proteins as well as to zinc binding species other than MTs. We found that upon exposure of HCEsv cells for 24 h with $^{68}ZnSO_4$, the concentration of zinc (^{nat}Zn+^{68}Zn) bound to MTs increased 4.45-fold when compared with control. The combination of $ZnSO_4$ and IL1α further increased the concentration of zinc in MTs approximately by 25% when compared with $^{68}ZnSO_4$ alone. Finally, the cytokine IL1α when added alone to HCEsv cells increased the concentration of zinc (^{nat}Zn) by 2.1-fold (Fig. 5 and Table 1).

Although the MALDI-TOF analysis revealed the presence of MTs in the fraction separated from SEC, a further separation was carried out by AEC coupled online with ICP-MS detector to separate MTs according to their isoelectric point. The SEC fraction containing MTs were collected, pre-concentrated, and injected to AEC-ICP-MS, and the levels of sulfur, zinc, copper, and cadmium were quantified following previous reports (27). The results obtained (see supplemental Tables 2 and 3) are in good agreement with the SEC results indicated in the above paragraph.

We also estimated by flow injection analysis (FIA-ICP-MS) the overall concentration of zinc, copper, and cadmium ele-

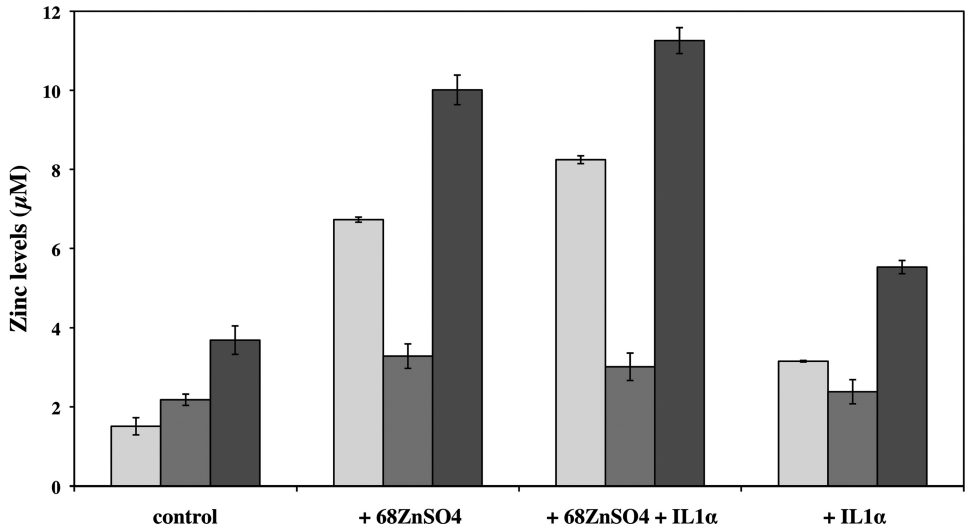

FIGURE 5. **Concentration of zinc (in μM) in MTs (*light gray bars*) and in species other than MTs (*dark gray bars*) in the cytosolic fraction of HCEsv cells.** Cultured HCEsv cells were either not treated (*control*) or exposed to $^{68}ZnSO_4$ and IL1α separately or in combination (*i.e.* ^{68}ZnSO4+IL1α) for 24 h. The total concentration of zinc bound to all zinc binding species including MTs (*black bars*) is also shown. Quantitative analysis was performed by IPD-HPLC-ICP-MS.

TABLE 1

Concentration of natural (^{nat}Zn) and "exogenous" zinc (^{68}Zn) found in zinc binding species (*i.e.*, MTs and other than MTs) in the cytosolic fraction of cells under control conditions (no treatment) and after exposure of cultured HCEsv cells to either (i) $^{68}ZnSO_4$ (100 μM), (ii) IL1α (100 units/ml), or (iii) a combination of $^{68}ZnSO_4$ (100 μM) and IL1α (100 units/ml) for 24 h

The concentration of total zinc in all "zinc binding species" reflects the sum of concentrations of zinc (^{nat}Zn + ^{68}Zn) bound to MTs and to other species distinct to MTs. The concentration of zinc in zinc binding species was determined by IPD-HLPC-ICP-MS.

Treatment	Zinc binding species	^{nat}Zn	^{68}Zn	Total zinc (^{nat}Zn+^{68}Zn)
		μM	μM	μM
Control	MTs	1.5 ± 0.2	0.0 ± 0.0	1.5 ± 0.2
	Other than MTs	2.2 ± 0.1	0.0 ± 0.0	2.2 ± 0.1
	All zinc binding species	3.7 ± 0.4	0.0 ± 0.0	3.7 ± 0.4
+$^{68}ZnSO_4$	MTs	0.48 ± 0.02	6.25 ± 0.04	6.7 ± 0.1
	Other than MTs	2.2 ± 0.2	1.1 ± 0.1	3.3 ± 0.3
	All zinc binding species	2.7 ± 0.2	7.3 ± 0.2	10.0 ± 0.4
+$^{68}ZnSO_4$ + IL1α	MTs	0.48 ± 0.04	7.77 ± 0.06	8.2 ± 0.1
	Other than MTs	1.7 ± 0.3	1.30 ± 0.09	3.0 ± 0.5
	All zinc binding species	2.2 ± 0.3	9.07 ± 0.03	11.3 ± 0.3
+IL1α	MTs	3.15 ± 0.02	0.0 ± 0.0	3.15 ± 0.02
	Other than MTs	2.4 ± 0.3	0.0 ± 0.0	2.4 ± 0.3
	All zinc binding species	5.5 ± 0.2	0.0 ± 0.0	5.5 ± 0.2

ments in whole HCEsv cell extracts (cytosolic and insoluble fractions) independently of the nature of the proteins to which these elements were bound. These results are shown in supplemental Tables 4 and 5 for cytosolic and insoluble fractions, respectively. We estimated that 83–93% of the total zinc in HCEsv cells was associated to zinc-binding proteins in the cytosolic fraction and the rest (7–17%) to the pellet.

Stoichiometry and Quantitation of MT Proteins in HCEsv Cells—The elemental stoichiometry of MTs under control conditions was S:Zn:Cu:Cd = 21:6:1:0 and S:Zn:Cu:Cd = 21:7:0:0 after exposure to zinc or IL1α. Thus, the element composition of MTs under control conditions was Zn_6Cu_1-MT and upon zinc or cytokine treatment was Zn_7-MT (supplemental Table 2).

Fig. 6 and Table 2 summarize the concentrations of MTs (expressed as μM) in the cytosolic fraction of HCEsv cells under control conditions (no treatment) and after exposure to zinc and IL1α. We estimated that more than 99% of all MT proteins detected in HCEsv cells were present in the cytosolic fraction. Under control conditions (no treatment), the concentration of zinc bound to MTs represented ~40% of the total zinc (^{nat}Zn+^{68}Zn) detected in all zinc-binding proteins in the soluble fraction. These results support the observation that the enhancement induced by $^{68}ZnSO_4$ in the gene expression of MTs in cultured HCEsv cells correlated with significant increases in MT proteins and bound zinc.

Inhibition of Transcription Prevents the Enhancement of MT Expression Induced by Zinc—To examine whether the effect of zinc on MT expression was regulated at the transcriptional or translational level, cultured HCEsv cells were pretreated for 30 min with either ActD, an inhibitor of transcription, or CH, an inhibitor of protein biosynthesis. This was followed by an exposure to $^{68}ZnSO_4$ for 24 h, at the end of which the concentrations of ^{nat}Zn and ^{68}Zn in MT proteins were determined. The results are shown in Fig. 7 and Table 3. Under steady-state conditions (control), ActD blocked the concentration of endogenous (native) MT protein by ~50%. However, in the presence of CH the total concentration of MTs was not significantly altered. Pretreatment of cultured HCEsv cells with the inhibitors before being exposed with $^{68}ZnSO_4$ (100 μM) for 24 h reduced the concentration of MT proteins by ~78% with ActD and ~40% by CH (Fig. 7 and Table 3). Approximately 90% of the total

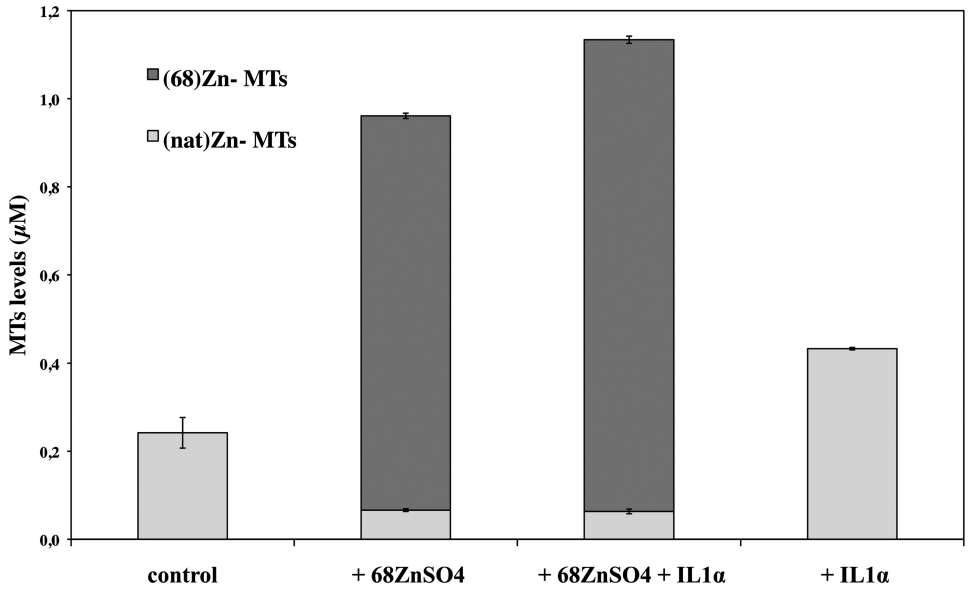

FIGURE 6. **Concentration of cellular MTs (in μM) in cultured HCEsv cells labeled with ^{nat}Zn or ^{68}Zn.** Cultured HCEsv cells were either not treated (*control*) or exposed to $^{68}ZnSO_4$ and IL1α separately or in combination (*i.e.* $^{68}ZnSO_4$ + IL1α) for 24 h. Quantitative analysis of MTs was performed by IPD-HPLC-ICP-MS.

TABLE 2

Concentration of MTs (μM) in HCEsv cells labeled with ^{nat}Zn and ^{68}Zn

Cells were cultured for 24 h in the absence (control) or presence of (i) $^{68}ZnSO_4$ (100 μM), (ii) IL1α (100 units/ml), and (iii) a combination of $^{68}ZnSO_4$ (100 μM) and IL1α (100 units/ml). The concentrations of MTs containing natural (^{nat}Zn) and "exogenous" zinc (^{68}Zn) were determined by IPD-HLPC-ICP-MS.

Treatment	^{nat}Zn-MTs	^{68}Zn-MTs	Total MTs
	μM	μM	μM
Control	0.24 ± 0.03	0.0 ± 0.0	0.24 ± 0.03
+$^{68}ZnSO_4$	0.066 ± 0.003	0.895 ± 0.006	0.96 ± 0.01
+$^{68}ZnSO_4$ + IL1α	0.063 ± 0.005	1.071 ± 0.008	1.13 ± 0.03
+IL1α	0.43 ± 0.03	0.0 ± 0.0	0.43 ± 0.03

concentration of MT proteins in HCEsv cells contained ^{68}Zn upon $^{68}ZnSO_4$ treatment, and the rest bonded with ^{nat}Zn. The pool of ^{68}Zn-labeled MT proteins consisted of MTs that originally contained ^{nat}Zn and had exchanged their bound metal ion for ^{68}Zn (~25%). The difference of ^{68}Zn-labeled MT proteins likely represented newly synthesized MTs, as 80% of the ^{68}Zn-labeled MT proteins were inhibited by ActD, and 45% were inhibited by CH.

DISCUSSION

This work presents a comprehensive microarray-based study on the differential gene expression profiling of multiple MT isoforms in tissues of the human eye. Further quantitative PCR analyses corroborated that multiple MT isoforms are expressed throughout the eye. Tissues in the anterior segment of the eye contained the highest levels of expression of MT1 and MT2 isoforms when compared with tissues in the posterior segment, including the retina, RPE, and sclera. The relative higher abundance of MT isoforms in cornea and lens may reflect their potential role in protective mechanisms against oxidative stress and inflammation; two of the physiological attributes associated to MTs. The cornea and lens constitute natural barriers within the anterior segment of the eye to external environmental insults including UV radiation. These tissues have developed defense systems (*i.e.* superoxide dismutases, glutathione peroxidases, catalases) against oxidative damage originating from the formation of reactive oxygen species, including H_2O_2, $^{\cdot}OH$, and O_2^- produced during the high metabolic activity in these and surrounding tissues (*i.e.* iris, ciliary body, trabecular meshwork).

In the human lens it has been shown that there is a spatial and isoform-specific cell distribution of MTs along the lens epithelium and lens fibers (38) and that the MT2A isoform is expressed in increased levels in lenses with age-related cataracts when compared with clear normal human lenses, suggesting a potential role in lens protection against oxidative stress (39).

The biological and biochemical significance of the multiple MT isoforms within the eye is not totally understood. The lack of specific antibodies for MT1 isoforms makes it difficult to assess their potential cell-specific distribution throughout the eye. Thus far, the cellular staining distribution observed within the corneal epithelium and endothelium with commercially available MT1/2 isoforms antibodies likely reflects a combination of the multiple MT1 isoforms expressed by these cells. However, MT3 antibodies stained retinal ganglion cells. In these cells the pattern of labeling was consistent with an intracellular staining of the cell bodies of ganglion cells and of the adjacent fiber bundles that form the nerve fiber layer (see supplemental Fig. 3). MT3 exhibits novel properties including the survival of neurons in culture and neuroprotection against toxic substances (40, 41). In the brain MT3 has been immunolocalized in astrocytes and neurons in cell bodies or along axons and dendrites (42, 43). Recent studies have shown that MT proteins secreted by astrocytes are rapidly internalized by retinal ganglion cells *in vivo*, promoting axonal regeneration (2). The cell-specific distribution of MT3 in the brain and retina may underlie biochemical and/or functional differences with other MT-specific isoforms. For example, it has been suggested that MT1 and MT2, but not MT3, are inducible at the transcriptional level by the heavy metals that they bind (44).

It is known that retinal ganglion cells are likely the first retinal cells to undergo cell death in glaucoma. These cells are

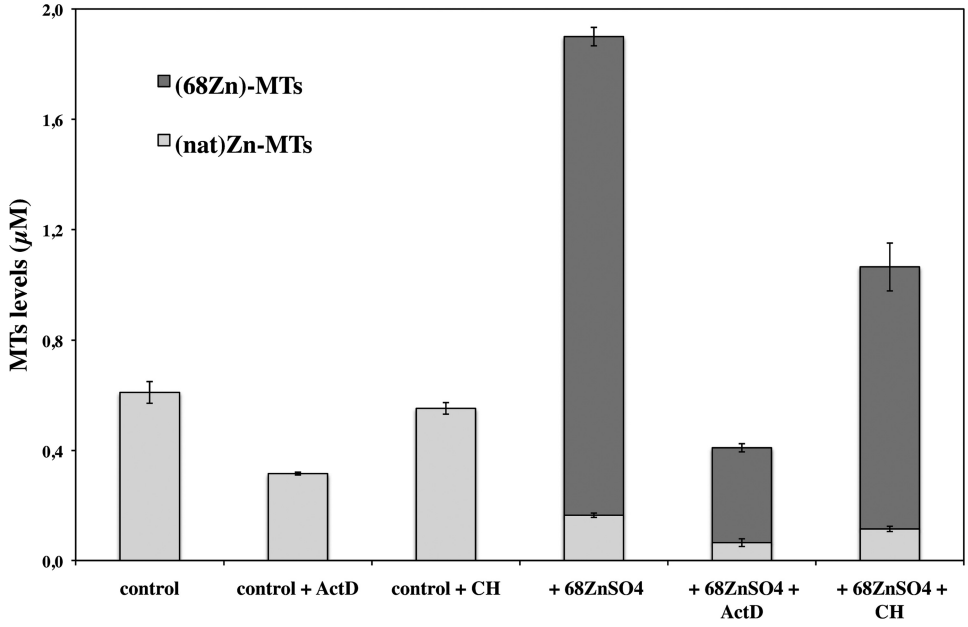

FIGURE 7. **Concentration of cellular MTs (in μM) labeled with ^{nat}Zn and ^{68}Zn in HCEsv cells.** Cultured HCEsv cells were pretreated for 30 min with either ActD or CH followed by exposure in the presence or absence of $^{68}ZnSO_4$ for 24 h. Quantitative analysis of MTs was performed by IPD-HPLC-ICP-MS.

TABLE 3

Effect of ActD and CH on the synthesis of MT proteins in cultured HCEsv cells in the presence or absence of $ZnSO_4$

HCEsv cells were exposed for 30 min to either ActD or CH followed of a 24-h treatment with $^{68}ZnSO_4$. The concentration of MTs (μM) containing natural (^{nat}Zn) and "exogenous" zinc (^{68}Zn) were determined by IPD-HLPC-ICP-MS.

Treatment	^{nat}Zn-MTs	^{68}Zn-MTs	Total MTs
	μM	μM	μM
Control	0.61 ± 0.04	0.0 ± 0.0	0.61 ± 0.04
Control + ActD	0.315 ± 0.005	0.0 ± 0.0	0.315 ± 0.005
Control + CH	0.55 ± 0.02	0.0 ± 0.0	0.55 ± 0.02
$+^{68}ZnSO_4$	0.164 ± 0.008	1.74 ± 0.03	1.90 ± 0.04
$+^{68}ZnSO_4$ + ActD	0.06 ± 0.01	0.34 ± 0.01	0.41 ± 0.03
$+^{68}ZnSO_4$ + CH	0.11 ± 0.01	0.95 ± 0.09	1.06 ± 0.09

highly sensitive to damage during oxidative stress or intense visible and UV light exposure. It has been shown that overexpression of MT1A in a human RPE cell line conferred protection against Cd^{2+} exposure, iron-induced oxidation, and UV light (45). The zinc concentration in the normal retina is elevated, and it is believed that zinc plays important roles in biochemical processes associated with the visual cycle, retinal cell survival, and the function of antioxidant enzymes (46). Under oxidative stress during light exposure, zinc can be released at high levels from the RPE cells and induce neuronal damage (47). In AMD, the accumulation of zinc can reach millimolar levels during druses formation in the subretinal space between the RPE and Bruch's membrane (48). It has been suggested that zinc and zinc-mediated processes may play a role in the development and progression of AMD, affecting the deposit and formation of druses. A large clinical trial evaluating the effect of zinc and antioxidants supplements (vitamins C and E and β-carotene) on the risk of progression to advanced AMD concluded that both zinc and antioxidants plus zinc, but not antioxidants alone, significantly reduced the progression of the neovascular form of AMD at intermediate and late stages of the disease (20).

Newsome *et al.* (49) undertook one of the first studies of the effects of oral zinc administration in AMD patients. In further studies Newsome *et al.* (50) documented that rats maintained on a zinc-deficient diet led to reduced MT levels in liver, retina, and RPE and an increased oxidative stress in the retina. On the other hand, when cultured RPE cells were set to grow under normal zinc levels, the intracellular MT level increased in response to oxidative stress insults, but it decreased under zinc-deficient conditions (50). Thus these results supported the view that increased cellular MT levels may confer higher protection against oxidative stress to a cell or tissue.

This work was carried out on a cultured human ocular cell line, HCEsv, capable of co-expressing multiple MT isoforms and inflammatory cytokines. It also permitted us to simultaneously examine the mechanisms by which zinc modulates their gene expression. Our data supported the assertion that zinc exerted a dual but antagonist effect on HCEsv cells, (i) a robust enhancement in the gene expression of MT isoforms and (ii) an inhibition of cytokine gene expression. It also suggested that cytokines (*i.e.* IL1α) were capable of enhancing the expression of MTs when added together with zinc, supporting the view that zinc mediates a cross-talk communication between MTs and inflammatory cytokines. This observation may be physiologically relevant as a number of ocular diseases, including AMD and glaucoma are associated with cell-mediated immune responses (51, 52).

It should not be totally ruled out whether zinc supplementation for reducing the risk of AMD progression may include up-regulation of MT and down-regulation of gene expression of proinflammatory cytokines. We think that one expected effect of zinc on MTs would be the reinforcement of the antioxidative status of targeted ocular tissues. Although the molecular mechanism by which zinc may inhibit cytokine expression in HCEsv cells has not been studied, in other cell systems it has been shown that zinc blocks the dimerization of Stat3 proteins

(53) or the activation of NF-κB by IkB (involved in signaling pathways linked to the expression of cytokines) by the activation of ILα and TNFα receptors, respectively.

It has been estimated that the total concentration of intracellular zinc ions in HP-29 cells is in the 200–300-μm range, and the concentration of "free" zinc ions (using the fluorogenic chelating agent FluoZin-3) is within the 600–800 pM range (54). This indicates that the concentration of intracellular free zinc is extremely low, and when not bound to zinc-binding proteins, it likely accumulates within mitochondria and secretory vesicles (zincosomes) (55, 56). It has been suggested that zinc is neurotoxic when released in excessive amounts (57). The uptake and release of zinc by cells involves membrane-bound zinc-transporter proteins. Thus far, two families of zinc transporters have been described; one involved in the export of zinc (*i.e.* SLC30A1 or ZnT-1) and another in the import of zinc (*i.e.* SLC39A1 or Zip1). Members of the two families are expressed in the ocular tissues examined in this work as well as HCEsv cells (data not shown). How these transporters regulate intracellular zinc ion concentration is currently unknown.

We applied an approach to quantitate the absolute concentrations of zinc-binding proteins and the concentration of zinc bound to MTs in cultured HCEsv cells under steady-state conditions and upon exposure to zinc and cytokinetic agent. The determination was carried out by HPLC-ICP-MS, a technique used extensively to quantitate MT levels in many tissues throughout the animal kingdom (37). This technique is based on the complete ionization of proteins and peptides into their elemental ions, allowing the detection and quantification of any hetero-element (any bioelement except carbon, hydrogen, nitrogen, and oxygen) present in a protein or in a protein-complex sample. Hetero-elements (*i.e.* Zn^{2+}, Cu^{+}, Cd^{2+}) are usually present in their natural form in many proteins, and their presence or absence may influence the function of those proteins. Because the type of information given by the ICP-MS technique is limited to the analytical determination of trace element concentrations and not to what specific proteins they are associated to, it is necessary to couple this procedure with a powerful separation technique such as HPLC. Thus, HPLC is used first to separate the proteins (*i.e.* cytosolic soluble proteins from cultured cells) in function of their molecular mass or isoelectric point. Then each fraction separated by HPLC is subjected to analytical ICP-MS and trace element speciation. In general, of all hybrid techniques, the coupling of HPLC with ICP-MS is one of the most widely used in the speciation analysis of essential elements in biological samples (58). Therefore, the hetero-element present in a protein of interest could be used as a tag in quantitative proteomics. ICP-MS allows simultaneous detection of multiple metallic elements and quantification of the abundance of isotopes of each element. The use of stable isotopes in connection with ICP-MS detection and appropriate mathematical calculations based on isotope dilution and IPD may also provide quantitative absolute concentrations of a protein and its hetero-element in a given sample. Because of the nature of the ICP-MS technique itself (*i.e.* it is an atomic technique), usually it is used in conjunction with MALDI-MS or ESI-MS techniques, allowing the identification and chemical characterization of the heteroatom-containing biomolecules (59).

Isolated MT is often heterogeneous in terms of its metal content and redox state. The metal content can differ among tissues and cells. Several biological factors may influence metal ion composition including tissue origin, age, and stage of development. In cells, MT may exist as a dynamic protein with different species depending on the state of the cells. The predominant species of MTs reported in cells are Zn_5-MT and Zn_6-MT, and they can reach up to micromolar concentrations (60). The stoichiometry of MT has been studied in purified proteins (37) or after extractions from tissues exposed to heavy metals (61, 62). Recent studies have suggested that under normal physiological conditions, MTs may exist in three states of thiols as metal-bound (MT), free (T, thionein), and disulfide (T_o, thionin) (63). However, the metal-MT stoichiometry under physiological conditions is presently unknown.

Our MT stoichiometry data provided additional insight information by showing that under steady-state conditions native MTs contained six zinc and one copper ions (Zn_6Cu_1-MT); however, when zinc or IL1α are added separately it favored the formation of Zn_7-MT species (see supplemental Table 2). The Zn_7-MT species likely do not exist in cells under control conditions because of the low affinity of MTs for the seventh zinc ion and the limited cellular availability of free zinc, which is estimated to be within the picomolar levels. However, upon stimulation of MT transcription and translation, the Zn_7-MT species become predominant. Previous reports have suggested that the zinc/MT stoichiometry depends on the total concentrations of both MT protein and zinc ions (4, 18, 54). This is consistent with our results. The robust increase in MT protein and zinc bound induced in cultured HCEsv cells upon exposure with exogenous zinc is consistent with the view that MTs are prone to fill all their zinc binding sites during *de novo* synthesis. We estimated that during this stimulation ~90% of the intracellular pool of MTs was loaded with exogenous ^{68}Zn ions, and the remaining 10% contained ^{nat}Zn. However, ~25% of the MTs containing ^{68}Zn resulted from zinc ion exchanged with ^{nat}Zn MTs. Thus, cells may have adapted to metal overloads by inducing a robust stimulation of MT protein synthesis to increase the metal binding capacity by occupying their seventh zinc ion site. Whether this scenario may occur *in vivo* waits to be investigated.

What are the biochemical implications of Zn_7MT species in HCEsv cells after zinc exposure? It is known that the MT affinity for zinc ions differs despite the tetrathiolate coordination environment for each of the seven zinc ions. Four of the zinc ions are bound tightly ($\log K = 11.8$), two are bound with intermediate strength ($\log K = 10$), and one is bound relatively weak ($\log K = 7.7$) (4). That the stability constant of one zinc atom (Zn_7) is significantly lower than the other six thermodynamically enables the release of one zinc atom from MT to other zinc-binding proteins. Thus, Zn_7-MT species has a greater antioxidant capacity than Zn_x-MT species (where x ranges from 0 to 6 zinc atoms). Our data suggest that when an excess of zinc is added, the MTs may interact more effectively with reactive oxygen species, decreasing the potential oxidative damage. We

predict that Zn_7-MT species likely will render the cell or tissue more resistant to oxidative stress insults.

Our results revealed that upon exposure of HCEsv cells with zinc, ~72.5% of the ^{nat}Zn-labeled MTs exchanged their bound metal element for ^{68}Zn. The remaining 27.5% of MTs appeared to conserve the ^{nat}Zn label. Another interesting observation is that during the time of exposure with zinc (24 h), the concentration of MTs proteins labeled with ^{68}Zn represented 93% of all the MTs detected in HCEsv cells and ~7% of MTs contained the ^{nat}Zn-bound metal. This finding suggested that ~80% of the total MTs in HCEsv cells exposed to zinc for 24 h were products of new synthesis.

This was supported by the effect of actinomycin on HCEsv cells before being exposed to zinc. This inhibitor of transcription prevented the enhancement of MTs induced by zinc. Interestingly, the concentration of ^{68}Zn binding MT proteins in the presence of actinomycin likely consisted not of newly synthesized proteins but rather of a small pool (27.5%) of ^{nat}Zn-binding proteins that exchanged their metal for ^{68}Zn. However, a smaller concentration (7%) of MTs were labeled with ^{nat}Zn and remained relatively constant in the presence or absence of actinomycin. Thus, it appears that a small concentration of MT proteins in HCEsv remains bound with ^{nat}Zn even though they are exposed for longer periods of times in an excess of ^{68}Zn.

In contrast, cycloheximide, an inhibitor of protein synthesis, only partially blocked the concentration of ^{68}Zn-bound MT proteins induced by zinc. We interpreted this result as the short and reversible effect of cycloheximide in blocking protein synthesis after its removal. Longer periods of pretreatment of HCEsv cells with cycloheximide led to cell death; thus, a 30-min pretreatment with cycloheximide followed by zinc exposure allowed HCEsv cells to recover partially to permit the induction of MT protein synthesis. This effect contrasted to the cellular tolerance and irreversible action of actinomycin during longer periods of time.

In summary, we have provided extensive information on the isoform tissue-specific profiling of MT gene expression in tissues of eye donors and have examined their regulation in an *in vitro* cell culture model. One of the novelties in this work was the use of array-based technology to analyze and compare simultaneously in a single cell system the effects of zinc and inflammatory interleukins on the expression of multiple MT isoforms. We applied IPD-HPLC-ICP-MS to (i) determine the stoichiometry of zinc binding sites per molecule of MT in HCEsv cells, (ii) metabolically follow the fate of zinc tracers (^{nat}Zn and ^{68}Zn) in MT proteins during the activation of HCEsv cells by zinc and cytokines, and (iii) quantitate the concentration of MTs proteins as well of the levels of the zinc tracers bound to MTs. Finally, we provide evidence that zinc ions mediate a cross-talk between MTs and cytokines to modulate their expression. These data may provide clues to explore the role of zinc in proinflammatory events and immune-regulated processes associated with eye diseases.

Acknowledgments—We thank Manuel Chacón for technical support and Carson Petrash for proofreading the manuscript.

REFERENCES

1. Thiersch, M., Raffelsberger, W., Frigg, R., Samardzija, M., Wenzel, A., Poch, O., and Grimm, C. (2008) Analysis of the retinal gene expression profile after hypoxic preconditioning identifies candidate genes for neuroprotection. *BMC Genomics* **9,** 73
2. Chung, R. S., Hidalgo, J., and West, A. K. (2008) New insight into the molecular pathways of metallothionein-mediated neuroprotection and regeneration. *J. Neurochem.* **104,** 14–20
3. Bell, S. G., and Vallee, B. L. (2009) The metallothionein/thionein system. An oxidoreductive metabolic zinc link. *Chembiochem.* **10,** 55–62
4. Li, Y., and Maret, W. (2008) Human metallothionein metallomics. *J. Anal. At. Spectrom.* **23,** 1055–1062
5. Penkowa, M., Giralt, M., Thomsen, P. S., Carrasco, J., and Hidalgo, J. (2001) Zinc or copper deficiency-induced impaired inflammatory response to brain trauma may be caused by the concomitant metallothionein changes. *J. Neurotrauma* **18,** 447–463
6. Gasull, T., Giralt, M., Hernandez, J., Martinez, P., Bremner, I., and Hidalgo, J. (1994) Regulation of metallothionein concentrations in rat brain. Effect of glucocorticoids, zinc, copper, and endotoxin. *Am. J. Physiol.* **266,** E760–E767
7. Carrasco, J., Hernandez, J., Gonzalez, B., Campbell, I. L., and Hidalgo, J. (1998) Localization of metallothionein-I and -III expression in the CNS of transgenic mice with astrocyte-targeted expression of interleukin 6. *Exp. Neurol.* **153,** 184–194
8. Penkowa, M., Moos, T., Carrasco, J., Hadberg, H., Molinero, A., Bluethmann, H., and Hidalgo, J. (1999) Strongly compromised inflammatory response to brain injury in interleukin-6-deficient mice. *Glia* **25,** 343–357
9. Quintana, A., Molinero, A., Florit, S., Manso, Y., Comes, G., Carrasco, J., Giralt, M., Borup, R., Nielsen, F. C., Campbell, I. L., Penkowa, M., and Hidalgo, J. (2007) Diverging mechanisms for TNF-α receptors in normal mouse brains and in functional recovery after injury. From gene to behavior. *J. Neurosci. Res.* **85,** 2668–2685
10. Pedersen, M. Ø., Larsen, A., Stoltenberg, M., and Penkowa, M. (2009) The role of metallothionein in oncogenesis and cancer prognosis. *Prog. Histochem. Cytochem.* **44,** 29–64
11. Vasák, M. (2005) Advances in metallothionein structure and functions. *J. Trace Elem. Med. Biol.* **19,** 13–17
12. Rigby Duncan, K. E., and Stillman, M. J. (2006) Metal-dependent protein folding. Metallation of metallothionein. *J. Inorg. Biochem.* **100,** 2101–2107
13. Romero-Isart, N., and Vasák, M. (2002) Advances in the structure and chemistry of metallothioneins. *J. Inorg. Biochem.* **88,** 388–396
14. Maret, W., and Krezel, A. (2007) Cellular zinc and redox buffering capacity of metallothionein/thionein in health and disease. *Mol. Med.* **13,** 371–375
15. Krezel, A., Hao, Q., and Maret, W. (2007) The zinc/thiolate redox biochemistry of metallothionein and the control of zinc ion fluctuations in cell signaling. *Arch. Biochem. Biophys.* **463,** 188–200
16. Vallee, B. L., and Falchuk, K. H. (1993) The biochemical basis of zinc physiology. *Physiol. Rev.* **73,** 79–118
17. Hao, Q., and Maret, W. (2005) Imbalance between pro-oxidant and pro-antioxidant functions of zinc in disease. *J. Alzheimers Dis.* **8,** 161–170
18. Colvin, R. A., Holmes, W. R., Fontaine, C. P., and Maret, W. (2010) Cytosolic zinc buffering and muffling. Their role in intracellular zinc homeostasis. *Metallomics* **2,** 306–317
19. Suemori, S., Shimazawa, M., Kawase, K., Satoh, M., Nagase, H., Yamamoto, T., and Hara, H. (2006) Metallothionein, an endogenous antioxidant, protects against retinal neuron damage in mice. *Invest. Ophthalmol. Vis. Sci.* **47,** 3975–3982
20. Age-Related Eye Disease Study Research Group (2001) A randomized, placebo-controlled, clinical trial of high-dose supplementation with vitamins C and E, β carotene, and zinc for age-related macular degeneration and vision loss. AREDS report no. 8. *Arch. Ophthalmol.* **119,** 1417–1436
21. Finamore, A., Devirgiliis, C., Panno, D., D'Aquino, M., Polito, A., Venneria, E., Raguzzini, A., Coudray, C., and Mengheri, E. (2005) Immune response in relation to zinc status, sex, and antioxidant defense in Italian elderly population. The ZENITH study. *Eur. J. Clin. Nutr.* **59,**

S68–S72
22. Mocchegiani, E., Malavolta, M., Marcellini, F., and Pawelec, G. (2006) Zinc, oxidative stress, genetic background, and immunosenescence. Implications for healthy ageing. *Immun. Ageing* **3,** 6
23. Cabreiro, F., Perichon, M., Jatje, J., Malavolta, M., Mocchegiani, E., Friguet, B., Petropoulos, I. (2008) Zinc supplementation in the elderly subjects. Effect on oxidized protein degradation and repair systems in peripheral blood lymphocytes. *Exp. Gerontol.* **43,** 483–487
24. Varin, A., Larbi, A., Dedoussis, G. V., Kanoni, S., Jajte, J., Rink, L., Monti, D., Malavolta, M., Marcellini, F., Mocchegiani, E., Herbein, G., and Fulop, T. Jr. (2008) *In vitro* and *in vivo* effects of zinc on cytokine signaling in human T cells. *Exp. Gerontol.* **43,** 472–482
25. Sanz-Medel, A., Montes-Bayón, M., del Rosario Fernández de la Campa M, Encinar, J. R., and Bettmer, J. (2008) Elemental mass spectrometry for quantitative proteomics. *Anal. Bioanal. Chem.* **390,** 3–16
26. Malavolta, M., Piacenza, F., Costarelli, L., Giacconi, R., Muti, E., Cipriano, C., Tesei, S., Speziab, S., and Mocchegiania, E. (2007) Combining UHR-SEC-HPLC-ICP-MS with flow cytometry to quantify metallothioneins and to study zinc homeostasis in human PBMC. *J. Anal. At. Spectrom.* **22,** 1193–1198
27. Maltez, H. F., Villanueva Tagle, M., Fernández de la Campa Mdel, R., and Sanz-Medel, A. (2009) Metal-metallothionein-like protein investigation by heteroatom-tagged proteomics in two different snails as possible sentinel organisms of metal contamination in freshwater ecosystems. *Anal. Chim. Acta* **650,** 234–240
28. Wang, R., Sens, D. A., Albrecht, A., Garrett, S., Somji, S., Sens, M. A., and Lu, X. (2007) Simple method for identification of metallothionein isoforms in cultured human prostate cells by MALDI-TOF/TOF mass spectrometry. *Anal. Chem.* **79,** 4433–4441
29. Sariego Muñiz, C., Marchante Gayón, J. M., García Alonso, J. I., and Sanz-Medel, A. (2001) Speciation of essential elements in human serum using anion-exchange chromatography coupled to post-column isotope dilution analysis with double focusing ICP-MS. *J. Anal. At. Spectrom.* **16,** 587–592
30. Schaumlöffel, D., Prange, A., Marx, G., Heumann, K. G., and Brätter, P. (2002) Characterization and quantification of metallothionein isoforms by capillary electrophoresis-inductively coupled plasma-isotope-dilution mass spectrometry. *Anal. Bioanal. Chem.* **372,** 155–163
31. Rodriguez-Cea, A., Fernández de la Campa, M. R., García Alonso, J. I., Sanz-Medel, A. (2003) Metal speciation analysis in eel (*Anguilla anguilla*) metallothioneins by anionic exchange-FPLC-isotope dilution-ICP-MS. *J. Anal. At. Spectrom.* **18,** 1357–1364
32. Martínez-Sierra, J. G., Moreno Sanz, F., Herrero Espílez, P., Santamaria-Fernandez, R., Marchante Gayón, J. M., and García Alonso, J. I. (2010) Evaluation of different analytical strategies for the quantification of sulfur-containing biomolecules by HPLC-ICP-MS. Application to the characterisation of ^{34}S-labeled yeast. *J. Anal. At. Spectrom.* **25,** 989–997
33. Meija, J. (2006) Mathematical tools in analytical mass spectrometry. *Anal. Bioanal. Chem.* **385,** 486–499
34. González Iglesias, H., Fernández Sánchez, M. L., García Alonso, J. I., and Sanz-Medel, A. (2007) Use of enriched ^{74}Se and ^{77}Se in combination with isotope pattern deconvolution to differentiate and determine endogenous and supplemented selenium in lactating rats. *Anal. Bioanal. Chem.* **389,** 707–713
35. González-Iglesias, H., Fernández-Sánchez, M. L., López-Sastre, J., and Sanz-Medel, A. (2012) Nutritional iron supplementation studies based on enriched ^{57}Fe added to milk in rats and isotope pattern deconvolution–ICP–MS analysis. *Electrophoresis*, in press
36. Benedicto, A., Hernández-Apaolaza, L., Rivas, I., and Lucena, J. J. (2011) Determination of 67Zn distribution in navy bean (*Phaseolus vulgaris* L.) after foliar application of ^{67}Zn-lignosulfonates using isotope pattern deconvolution. *J. Agric. Food Chem.* **59,** 8829–8838
37. Prange, A., and Schaumlöffel, D. (2002) Hyphenated techniques for the characterization and quantification of metallothionein isoforms. *Anal. Bioanal. Chem.* **373,** 441–453
38. Oppermann, B., Zhang, W., Magabo, K., and Kantorow, M. (2001) Identification and spatial analysis of metallothioneins expressed by the adult human lens. *Invest. Ophthalmol. Vis. Sci.* **42,** 188–193
39. Kantorow, M., Kays, T., Horwitz, J., Huang, Q., Sun, J., Piatigorsky, J., and Carper, D. (1998) Differential display detects altered gene expression between cataractous and normal human lenses. *Invest. Ophthalmol. Vis. Sci.* **39,** 2344–2354
40. Uchida, Y., Gomi, F., Masumizu, T., and Miura, Y. (2002) Growth inhibitory factor prevents neurite extension and the death of cortical neurons caused by high oxygen exposure through hydroxyl radical scavenging. *J. Biol. Chem.* **277,** 32353–32359
41. Yu, W. H., Lukiw, W. J., Bergeron, C., Niznik, H. B., and Fraser, P. E. (2001) Metallothionein III is reduced in Alzheimer disease. *Brain Res.* **894,** 37–45
42. Masters, B. A., Quaife, C. J., Erickson, J. C., Kelly, E. J., Froelick, G. J., Zambrowicz, B. P., Brinster, R. L., and Palmiter, R. D. (1994) Metallothionein III is expressed in neurons that sequester zinc in synaptic vesicles. *J. Neurosci.* **14,** 5844–5857
43. Yamada, M., Hayashi, S., Hozumi, I., Inuzuka, T., Tsuji, S., and Takahashi, H. (1996) Subcellular localization of growth inhibitory factor in rat brain. Light and electron microscopic immunohistochemical studies. *Brain Res.* **735,** 257–264
44. Zangger, K., and Armitage, I. M. (2004) in *Handbook of Metalloproteins* (Messerschmidt, A., Bode, W., and Cygler, M., eds.) Vol. 3, pp. 353–364, John Wiley & Sons, Chichester, UK
45. Lu, H., Hunt, D. M., Ganti, R., Davis, A., Dutt, K., Alam, J., and Hunt, R. C. (2002) Metallothionein protects retinal pigment epithelial cells against apoptosis and oxidative stress. *Exp. Eye Res.* **74,** 83–92
46. Galin, M. A., Nano, H. D., and Hall, T. (1962) Ocular zinc concentration. *Invest. Ophthalmol.* **1,** 142–148
47. Ugarte, M., and Osborne, N. N. (2001) Zinc in the retina. *Prog. Neurobiol.* **64,** 219–249
48. Lengyel, I., Flinn, J. M., Peto, T., Linkous, D. H., Cano, K., Bird, A. C., Lanzirotti, A., Frederickson, C. J., and van Kuijk, F. J. (2007) High concentration of zinc in sub-retinal pigment epithelial deposits. *Exp. Eye Res.* **84,** 772–780
49. Newsome, D. A., Swartz, M., Leone, N. C., Elston, R. C., and Miller, E. (1988) Oral zinc in macular degeneration. *Arch. Ophthalmol.* **106,** 192–198
50. Miceli, M. V., Tate, D. J., Jr., Alcock, N. W., and Newsome, D. A. (1999) Zinc deficiency and oxidative stress in the retina of pigmented rats. *Invest. Ophthalmol. Vis. Sci.* **40,** 1238–1244
51. Anderson, D. H., Mullins, R. F., Hageman, G. S., and Johnson, L. V. (2002) A role for local inflammation in the formation of drusen in the aging eye. *Am. J. Ophthalmol.* **134,** 411–431
52. Wax, M. B., and Tezel, G. (2009) Immunoregulation of retinal ganglion cell fate in glaucoma. *Exp. Eye Res.* **88,** 825–830
53. Kitabayashi, C., Fukada, T., Kanamoto, M., Ohashi, W., Hojyo, S., Atsumi, T., Ueda, N., Azuma, I., Hirota, H., Murakami, M., and Hirano, T. (2010) Zinc suppresses Th17 development via inhibition of STAT3 activation. *Int. Immunol.* **22,** 375–386
54. Krezel, A., and Maret, W. (2006) Zinc-buffering capacity of a eukaryotic cell at physiological pZn. *J. Biol. Inorg. Chem.* **11,** 1049–1062
55. Murgia, C., Vespignani, I., Cerase, J., Nobili, F., and Perozzi, G. (1999) Cloning, expression, and vesicular localization of zinc transporter Dri 27/ZnT4 in intestinal tissue and cells. *Am. J. Physiol.* **277,** G1231–G1239
56. Murgia, C., Grosser, D., Truong-Tran, A. Q., Roscioli, E., Michalczyk, A., Ackland, M. L., Stoltenberg, M., Danscher, G., Lang, C., Knight, D., Perozzi, G., Ruffin, R. E., and Zalewski, P. (2011) Apical localization of zinc transporter ZnT4 in human airway epithelial cells and its loss in a murine model of allergic airway inflammation. *Nutrients* **3,** 910–928
57. Sensi, S. L., and Jeng, J. M. (2004) Rethinking the excitotoxic ionic milieu. The emerging role of Zn^{2+} in ischemic neuronal injury. *Curr. Mol. Med.* **4,** 87–111
58. Bettmer, J. (2010) Application of isotope dilution ICP-MS techniques to quantitative proteomics. *Anal. Bioanal. Chem.* **397,** 3495–3502
59. Szpunar, J. (2005) Advances in analytical methodology for bioinorganic speciation analysis. Metallomics, metalloproteomics, and heteroatom-tagged proteomics and metabolomics. *Analyst* **130,** 442–465
60. Krezel, A., and Maret, W. (2007) Dual nanomolar and picomolar Zn(II) binding properties of metallothionein. *J. Am. Chem. Soc.* **129,**

10911–10921
61. Połec, K., Peréz-Calvo, M., García-Arribas, O., Szpunar, J., Ribas-Ozonas, B., and Lobinski, R. (2002) Investigation of metal complexes with metallothionein in rat tissues by hyphenated techniques. *J. Inorg. Biochem.* **88,** 197–206
62. Goenaga-Infante, H., Van Campenhout, K., Blust, R., and Adams, F. C. (2002) Inductively coupled plasma time-of-flight mass spectrometry coupled to high performance liquid chromatography for multielemental speciation analysis of metalloproteins in carp cytosols. *J. Anal. At. Spectrom.* **17,** 79–97
63. Krezel, A., and Maret, W. (2007) Different redox states of metallothionein/thionein in biological tissue. *Biochem. J.* **402,** 551–558